

Bottom electrode crystallization of $\text{Pb}(\text{Zr},\text{Ti})\text{O}_3$ thin films made by RF magnetron sputtering

This article has been downloaded from IOPscience. Please scroll down to see the full text article.

2005 J. Phys.: Condens. Matter 17 7263

(<http://iopscience.iop.org/0953-8984/17/46/010>)

View [the table of contents for this issue](#), or go to the [journal homepage](#) for more

Download details:

IP Address: 129.252.86.83

The article was downloaded on 28/05/2010 at 06:46

Please note that [terms and conditions apply](#).

Bottom electrode crystallization of $\text{Pb}(\text{Zr}, \text{Ti})\text{O}_3$ thin films made by RF magnetron sputtering

A I Mardare^{1,2}, C C Mardare^{1,2}, J R A Fernandes^{1,3},
J Agostinho Moreira^{2,4} and M B Marques^{1,2}

¹ UOSE-INESC-Porto, Rua do Campo Alegre 687, 4169-007, Porto, Portugal

² Departamento de Física, Universidade do Porto, Rua do Campo Alegre 687, 4169-007, Porto, Portugal

³ Departamento de Física, Universidade de Trás-os-Montes e Alto Douro, 5001-911, Vila Real, Portugal

⁴ IFIMUP, Rua do Campo Alegre 687, 4169-007, Porto, Portugal

E-mail: amardare@fc.up.pt

Received 30 June 2005

Published 1 November 2005

Online at stacks.iop.org/JPhysCM/17/7263

Abstract

The bottom electrode crystallization method was used for the heat-treatment of amorphous $\text{Pb}(\text{Zr}_{0.52}, \text{Ti}_{0.48})\text{O}_3$ thin films deposited by radio-frequency magnetron sputtering on Pt/Ti/SiO₂/Si substrates. Two different heating and cooling rates were applied and two different contact wires (W and Pt) were alternately used for the Joule heat generation in the Pt bottom electrode. The dielectric and ferroelectric properties of the films were compared with the properties of the films crystallized using halogen lamp annealing in the same conditions. All the PZT samples showed similar ferroelectric properties at room temperature, with high dielectric constant and remanent polarization values as well as good resistance to ferroelectric fatigue, the Al/PZT/Pt/Ti/SiO₂/Si capacitors having low leakage currents. The experimental results obtained show that the bottom electrode crystallization method is a cheap and low power consumption method which can successfully replace the classical crystallization methods.

1. Introduction

In the last decades, there have been intensive studies regarding the use of the ferroelectric lead zirconate titanate (PZT) for memory devices, such as ferroelectric non-volatile memory (FeRAM) and dynamic random access memory (DRAM). Different deposition methods [1–4], bottom electrode materials ((La, Sr)CoO₃ [5], Ir [6] and LaNiO₃ [7]) and crystallization methods [8–10] have been investigated for improving the ferroelectric properties of PZT thin films. Recently, a new crystallization method which uses the metallic bottom electrode as a heating element has been developed. This bottom electrode crystallization (BEC) method

allows a wide range of heating and cooling rates, from very slow ones (furnace-like) up to very fast ones (rapid-thermal-annealing-like) [11, 12].

Platinum is the most widely used material for bottom electrodes in ferroelectric capacitors having high electrical conductivity, good stability to oxidation at high temperatures and high Schottky barrier height, which allows the fabrication of capacitors with low leakage current values. The possibility of using Pt as resistive heating element for heat-treatments of thin films has already been exploited for the crystallization of PZT thin films deposited by laser ablation [13, 14], but a detailed study regarding the properties of PZT thin films deposited by radio-frequency (RF) magnetron sputtering and crystallized by the BEC method has not been reported yet to the best of our knowledge.

The aim of the present work is the investigation of PZT thin film capacitor properties deposited by the RF magnetron sputtering technique and crystallized by the BEC method. A comparison regarding the ferroelectric properties of PZT films obtained by different methods (BEC and RTA) was also made.

2. Experimental details

(100) oriented silicon wafers were cut in $1 \times 1.5 \text{ cm}^2$ pieces to be used as substrates. After cleaning and heat-treating at 950°C in a tubular furnace in O_2 flow for 72 h, a layer of approximately $1 \mu\text{m}$ thick SiO_2 was obtained. The oxidized substrates were coated with PZT/Pt/Ti thin films, all the layers being deposited by RF magnetron sputtering in Ar at 1×10^{-2} mbar, using 2 inch diameter targets. The metallic film thicknesses were measured in real time during deposition using a quartz thickness monitor. Before each deposition sequence, the chamber was evacuated to a base pressure of at least 10^{-6} mbar.

The 30 nm thick Ti films were made *in situ* at 200°C , using an RF power of 150 W. The 200 nm thick Pt films were deposited on top of the Ti layer at 500°C using the same power of 150 W and without breaking the vacuum between depositions. For depositing the PZT thin films a sintered oxide target with the morphotropic composition of $\text{Zr}/\text{Ti} = 52/48$ and with 10 mol% Pb excess was used. The PZT films were deposited at room temperature for 1 h, using an RF power of 100 W. In this case a lower RF power was used to avoid the target damage. Before each deposition, the targets were pre-sputtered for about 15 min in order to avoid contamination and to have a reproducible stoichiometry.

The PZT films were crystallized in air for 10 min at 650°C using BEC and halogen lamp methods. In both cases, two different heating and cooling rates were used (1 and 10°C s^{-1}). The BEC method was used for crystallizing two series of samples having two different pairs of contact wires (W and Pt). The contact wires were placed on the surface of the Pt film at a distance of 1.1 cm from each other. Table 1 summarizes the conditions used for the crystallization of the PZT thin films. A 3.5 A current source was used for applying DC currents to the Pt films. The annealing process was controlled by a computer running a LabView[®] program using a proportional-integral-differential (PID) controller. The thickness of the PZT films measured after crystallization using a profilometer (Dektak IIA) was 400 nm. For the electrical characterization of the films, Al top electrodes with an area of 0.1 mm^2 were deposited by thermal evaporation using a shadow mask.

The crystalline phases and the preferential orientation of the PZT thin films were determined by the x-ray diffraction method using a Siemens D5000 diffractometer. The surface morphology of the films was studied using a scanning electron microscope (SEM) Philips/FEI Quanta 400. The evaluation of the capacitor leakage currents was carried out with a Keithley 487 picoammeter. The samples were poled using a 200 kV cm^{-1} electric field for 10 s, 10 min before starting the measurements, in order to allow time for the capacitors to discharge; the

Table 1. Conditions for the crystallization of the PZT thin films.

Sample name	Crystallization method	Contact wires	Heating/cooling rates (°C s ⁻¹)
Pt 1	BEC	Pt	1
Pt 10			10
W 1		W	1
W 10			10
H 1	Halogen	—	1
H 10	Lamps	—	10

current measurements were performed 5 s after each 0.5 V increase in the voltage. The capacitance as a function of applied bias voltage was recorded using an HP4192A impedance analyser. The probing AC signal used had 5 mV amplitude and its frequency was 10 kHz. A system composed of an amplifier, a function generator HP 8116A and a LeCroy 9310M oscilloscope was used for recording the ferroelectric hysteresis loops and the ferroelectric fatigue of the capacitors.

3. Results and discussion

The thermal energy necessary for the PZT crystallization using the BEC method is obtained by the Joule effect in the Pt film and in the electrical contact regions. The contact resistances depend on the current carrying wire material and may influence the overall system behaviour. The room temperature resistance of different electrical contacts can be easily estimated by measuring the electrical resistivity of the Pt film ($2 \times 10^{-5} \Omega \text{ cm}$) followed by the calculation of its resistance and by measuring the total resistance of the system (Pt film and contacts). When W contact wires were used, the room temperature electrical resistance of the Pt film and contacts was around 2.5 Ω , while when Pt wires were used the measured total resistance was decreased to around 1.2 Ω . Using these values, the contact resistance for the Pt and W wires was estimated to be around 0.12 and 0.77 Ω respectively.

Figure 1 shows the SEM images of the Pt surface in the electrical contact regions when W and Pt contact wires were used. When using Pt wires (figure 1(a)), pieces of the wire remained on the surface of the film after the removal of the contacts, most probably due to the sintering of the Pt wire and Pt film at high temperatures, confirming the small contact resistance obtained. When W wires were used (figure 1(b)), small contact imperfections led to the forming of localized high current densities under the W wire, which ultimately had as a result the complete evaporation of all the layers deposited on the silicon substrate and a greater contact resistance.

In figure 2 are shown the x-ray diffractograms for all the PZT films crystallized with different methods and heating/cooling rates. All the PZT peaks belong to the perovskite phase and no pyrochlore phase could be observed. One can see that the PZT films had no preferential orientation and very small differences can be observed between the diffractograms obtained from different samples. This result suggests that both methods (BEC and halogen lamps) used for the crystallization of the PZT thin films produce similar results with no significant changes in the crystalline orientations due to the different heating and cooling rates for the given crystallization time (10 min at 650 °C).

The surface morphology of the PZT thin films presents similar properties for different crystallization conditions as shown in figure 3. The surface of all PZT films is relatively

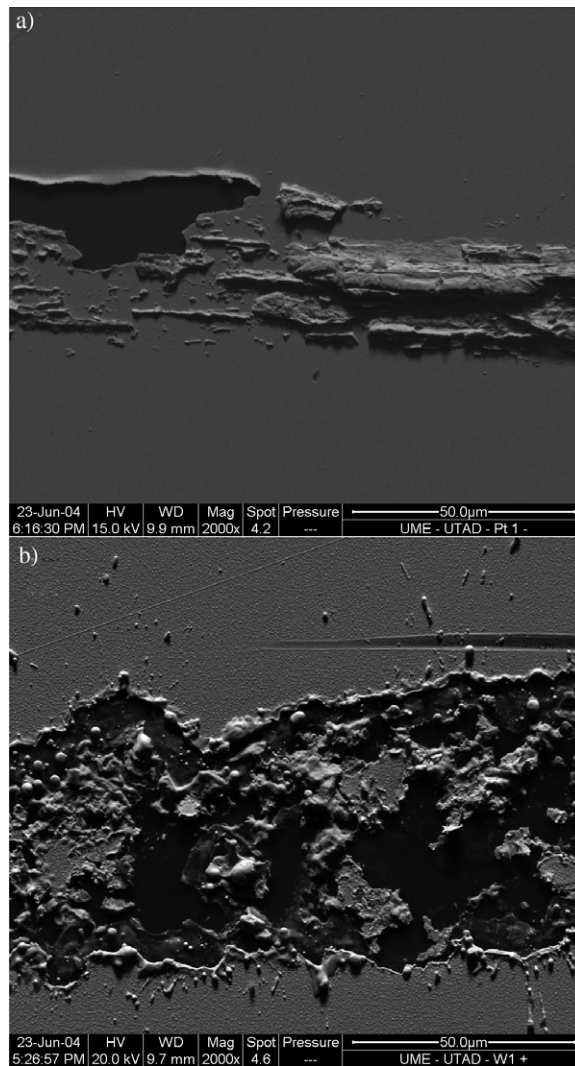


Figure 1. SEM images of the electrical contact regions on the surface of the Pt films when Pt (a) and W (b) wires were used for the BEC of PZT thin films.

smooth, grains with a size of maximum 500 nm being observed in all the films. In the case of the PZT samples crystallized using halogen lamps, one can observe the presence of charge accumulations localized in the grain boundary regions which led to the appearance of artefacts in the SEM image (white droplets of maximum 300 nm in diameter). For the PZT samples crystallized using the BEC method no charge effects were visible on the surface of the films, most likely due to the DC current passing through the bottom electrode during crystallization.

The PZT capacitor leakage current curves are shown in figure 4. In the case of PZT thin films crystallized using fast heating rates ($10^{\circ}\text{C s}^{-1}$) one can observe that the leakage current density curves measured on the PZT films crystallized by BEC are similar to the values measured on the PZT films crystallized using halogen lamps. In this situation, different contact wires used for BEC do not appear to modify significantly the leakage currents of the PZT films

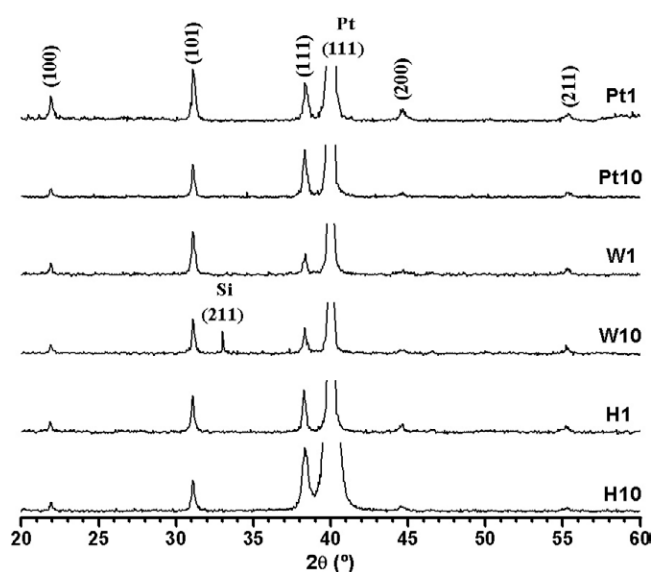


Figure 2. X-ray diffraction graphs for the PZT thin films heat-treated with different methods and heating/cooling rates.

when compared with halogen lamp annealing. For the PZT films crystallized using slow heating rates ($1\text{ }^{\circ}\text{C s}^{-1}$), the PZT crystallized with the halogen lamps shows higher leakage currents at high electric fields than the other samples. From the point of view of low voltage applications, one can observe that none of the PZT films present leakage current densities higher than 10^{-6} A cm^{-2} for an applied field of 400 kV cm^{-1} .

The capacitance and the real part of the complex dielectric constant of the PZT films as a function of the applied voltage are shown in figure 5. The measurements were performed with a DC-voltage bias swept from 12 to -12 V and back again; arrows indicate the sweep direction. The observed hysteresis loops and the peak occurrence are characteristic of reversal polarization due to domain switching. The difference in the maximum values of the intensities and the absolute position of the peaks is usually interpreted as originating in different environments of the bottom electrodes, and differences in the work functions and stress [15]. The asymmetrical behaviour of the C - V curves is attributed to an asymmetrical electrode structure of the samples (Al top and Pt bottom electrodes). One can observe that the capacitances measured for the PZT films crystallized by halogen lamps are smaller than the corresponding values obtained from PZT films crystallized by the BEC method. This is probably due to the charge accumulation in the PZT capacitors crystallized by halogen lamps, as observed in figure 3.

Comparing the capacitances measured in each sample for different heating rates, one can observe that all the PZT films crystallized using fast heating rates ($10\text{ }^{\circ}\text{C s}^{-1}$) showed higher capacitances for an applied voltage corresponding to the coercive field than the ones measured in the films crystallized using low heating rates. This can be attributed to the increased Ti out-diffusion and oxidation on the surface of the Pt electrodes, resulting in the formation of a low dielectric constant interfacial layer in the case of using low heating rates, due to longer time exposure to high temperatures [16]. However, when BEC was used for the crystallization of the PZT films, the differences between the C - V curves were attenuated, and in the case of using Pt contact wires the films crystallized with different heating rates showing almost identical C - V curves. An explanation for these differences between the PZT samples would

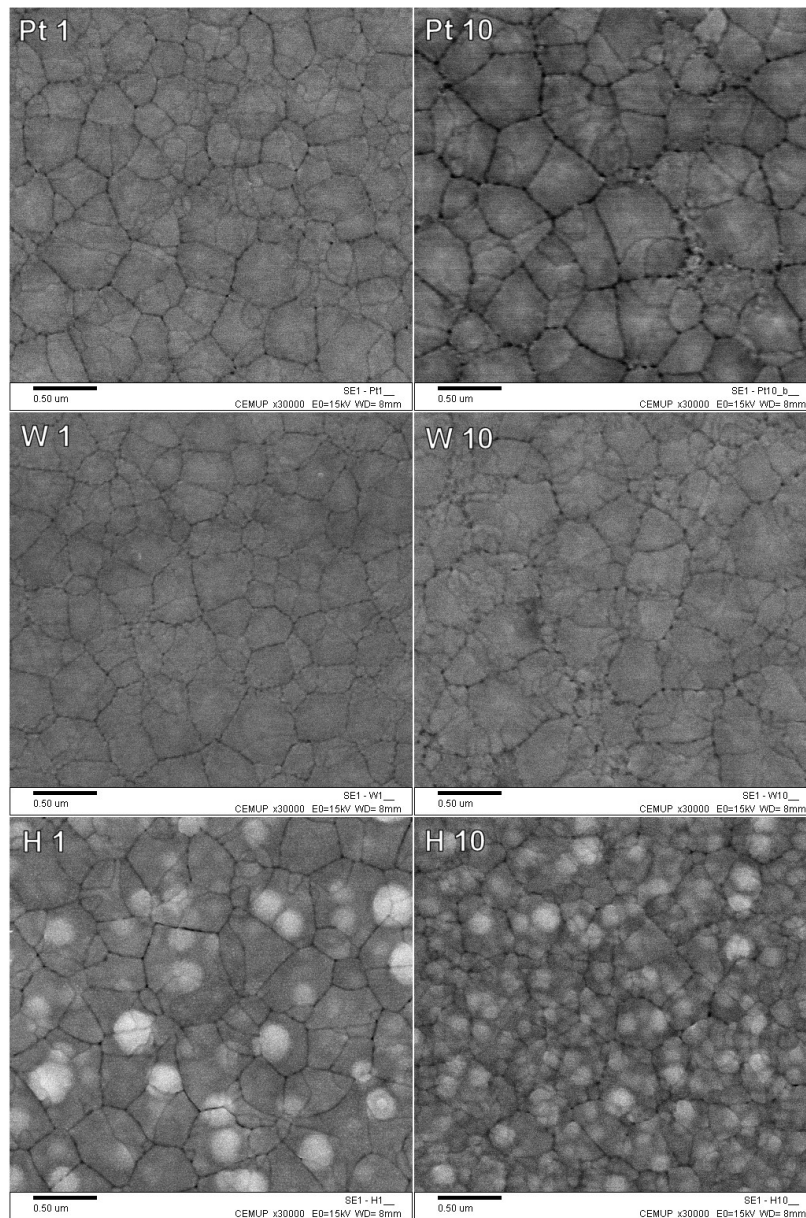


Figure 3. SEM images of the surface of PZT thin films crystallized using different methods and heating/cooling rates.

be a decreased Ti diffusion in the case of using BEC for the heat-treatments, having as a result the presence of a much thinner low dielectric constant layer and a corresponding increase in the total capacitance [17]. The fact that at the maximum applied voltage (both positive and negative) the capacitance differs significantly as a function of the heating rates when halogen lamps were used for the PZT crystallization also indicates the presence of a low dielectric constant layer which is barely noticeable from this point of view when the BEC method was used [18].

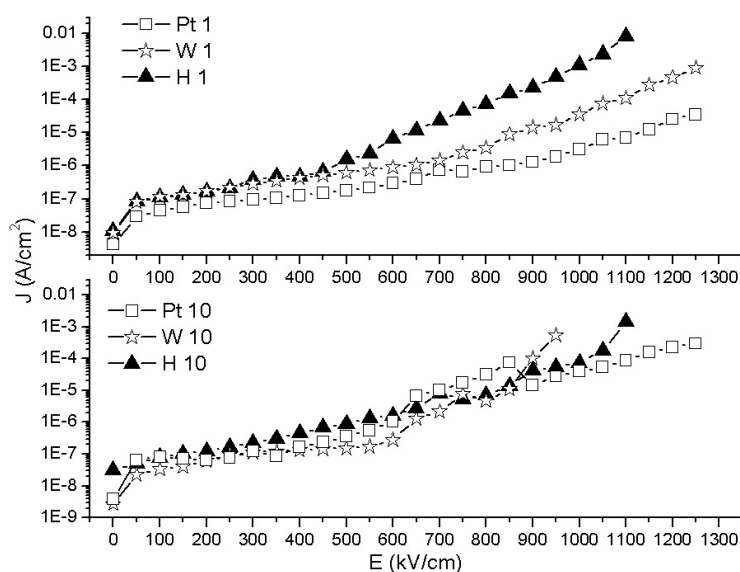


Figure 4. Leakage current curves of the PZT capacitors with the PZT films crystallized using different conditions.

The electric polarization versus applied field hysteresis loops measured for all the PZT samples are shown in figure 6. In the case of using fast heating rates for the PZT crystallization, one can see that all the ferroelectric responses are similar, the PZT films having remanent polarizations of around $15 \mu\text{C cm}^{-2}$ and coercive fields of around 100 kV cm^{-1} . From the hysteresis loops for the PZT films crystallized using slow heating rates one can observe that the use of BEC with Pt contact wires and the use of halogen lamps gave identical results, having a coercive field of around 200 kV cm^{-1} . The use of BEC with W contact wires had as a result a decrease in the value of the remanent polarization of around 25%, and in this case the coercive field was comparable with the PZT films crystallized using fast heating rates. Using slow heating rates, a maximum remanent polarization of $25 \mu\text{C cm}^{-2}$ was obtained.

An important feature of the ferroelectric capacitors is the ferroelectric fatigue which represents the decrease of the remanent polarization values as a function of the number of electric field switching cycles. In figure 7 are presented the ferroelectric fatigue curves measured in all PZT samples for switching cycles up to 10^{10} . One can observe that no significant differences can be observed when comparing the fatigue of the PZT films crystallized using the same heating rates and different methods. For both fast and slow heating rates, the samples crystallized with the lamps and the ones crystallized by the BEC method with Pt contact wires showed almost identical results, the PZT films showing a maximum decay of the remanent polarization of 25% of their initial values (samples Pt 1 and H 1). When PZT was crystallized by BEC with W contact wires, for slow heating rates the decay of the remanent polarization was around 15% whereas for the fast heating rates after 10^8 switching cycles a severe degradation of the electrodes occurred leading to the increase of the leakage currents, the widening of the hysteresis loops and the recording of a fake increased remanent polarization.

4. Conclusions

Using the bottom electrode crystallization method and the halogen lamp annealing, PZT thin films deposited by RF magnetron sputtering were crystallized in air for 10 min at 650°C using

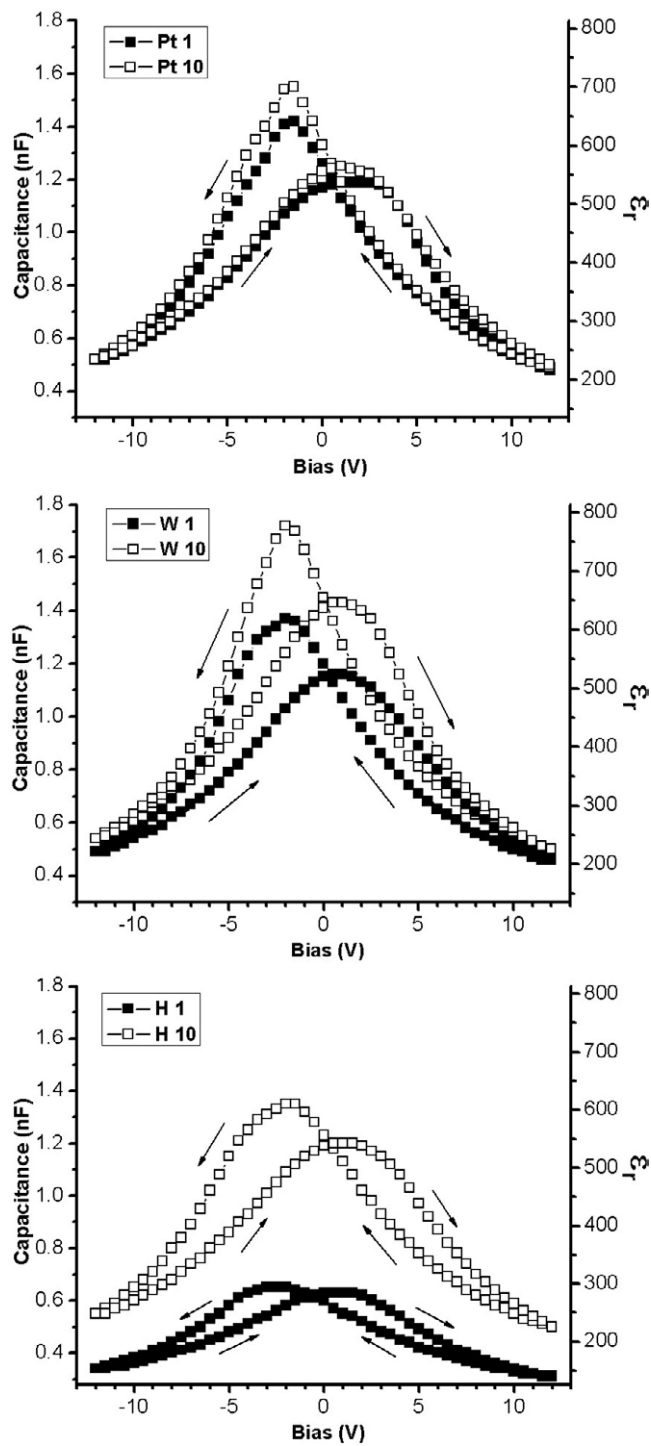


Figure 5. Capacitance and the real part of the complex dielectric constant versus applied voltage for the PZT thin film capacitors.

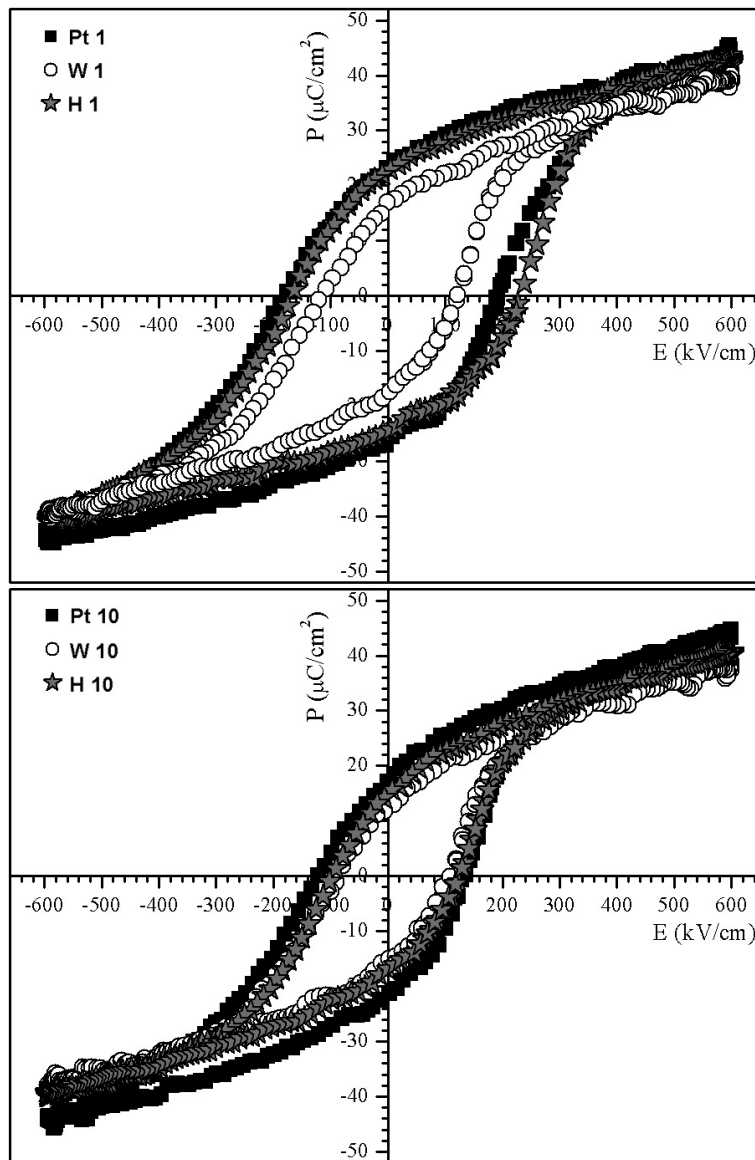


Figure 6. Hysteresis loops for the PZT thin films crystallized in different conditions.

two different heating and cooling rates. The BEC method was used with two different contact wires (Pt and W) and the crystallographic, morphologic, electrical and ferroelectric properties of the films were presented in comparison with the PZT thin films crystallized by halogen lamps. The measurements showed similar and in some cases slightly improved properties for the PZT films crystallized by BEC when compared with the ones crystallized by halogen lamps. The BEC method remains an interesting and useful way for obtaining heat treatments of thin films and may represent the starting point for further studies involving the crystallization of other different thin film materials.

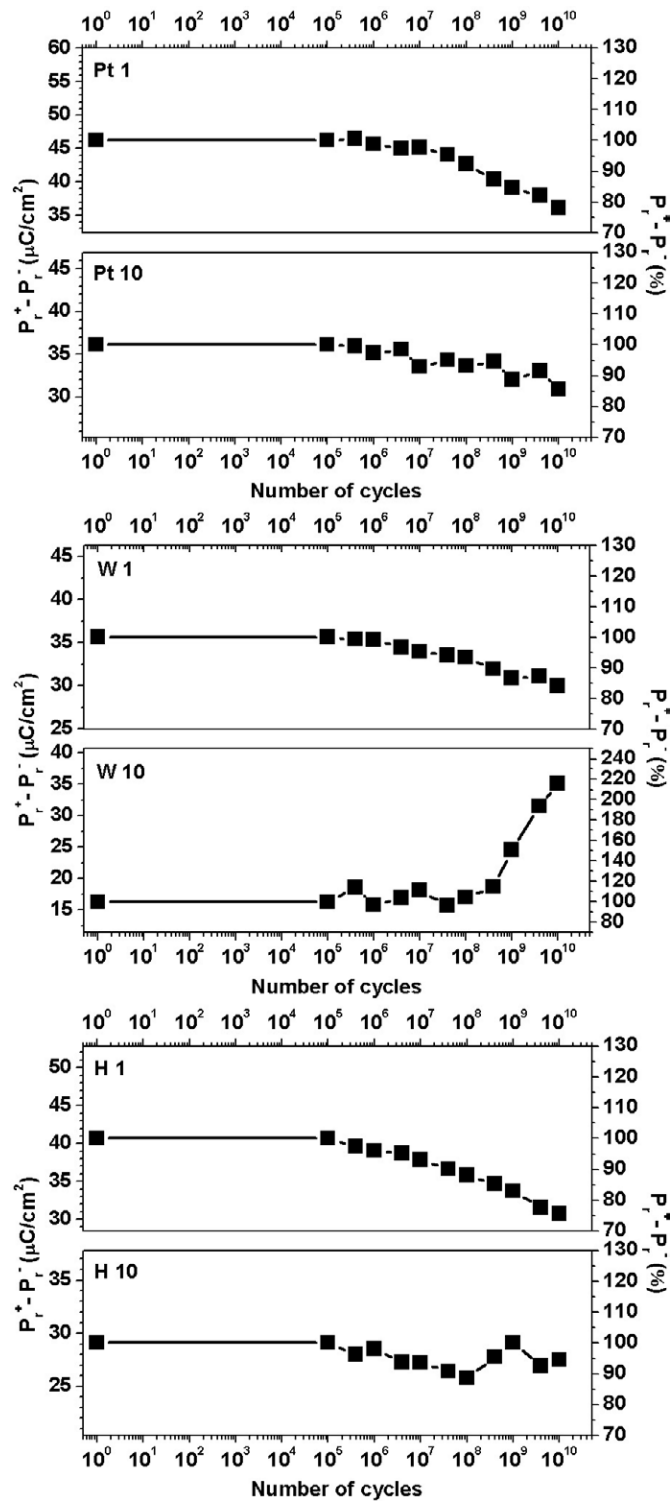


Figure 7. Ferroelectric fatigue of the PZT thin films crystallized in different conditions.

Acknowledgment

A I Mardare and C C Mardare would like to acknowledge the Portuguese Foundation for Science and Technology (FCT) for Financial support through the grants SFRH/BO/11374/2002 and SFRH/DB/12454/2003 respectively.

References

- [1] Chang C C and Chen K H 1999 *J. Mater. Sci., Mater. Electron.* **10** 551
- [2] Wang Z-J, Maeda R, Ichiki M and Kokawa H 2001 *Japan. J. Appl. Phys.* **40** 5523
- [3] Cheng J and Meng Z 2000 *J. Mater. Sci. Lett.* **19** 1945
- [4] Zai M H M, Akiba A, Goto H, Matsumoto M and Yeatman E M 2001 *Thin Solid Films* **394** 97
- [5] Im K V, Kuh B J, Park S O, Lee S I and Choo W K 2000 *Japan. J. Appl. Phys.* **39** 5437
- [6] Nakamura T, Nakao Y, Kamisawa A and Takasu H 1995 *Japan. J. Appl. Phys.* **34** 5184
- [7] Wakiya N, Azuma T, Shinozaki K and Mizutani N 2002 *Thin Solid Films* **410** 114
- [8] Vasant Kumar C V R, Pascual R and Sayer M 1992 *J. Appl. Phys.* **71** 864
- [9] Chen J, Udayakumar K R, Brooks K G and Cross L E 1992 *J. Appl. Phys.* **71** 4465
- [10] Yamakawa K, Imai K, Arisumi O, Arikado T, Yoshioka M, Owada T and Okumura K 2002 *Japan. J. Appl. Phys.* **41** 2630
- [11] Joanni E, Mardare A I, Mardare C C and Fernandes J R A 2003 *Japan. J. Appl. Phys.* **42** L863
- [12] Joanni E, Mardare A I, Mardare C C and Marques M B 2004 *Rev. Sci. Instrum.* **75** 2950
- [13] Mardare A I, Mardare C C and Joanni E 2005 *J. Eur. Ceram. Soc.* **25** 735
- [14] Mardare A I, Mardare C C, Pinheiro E and Joanni E 2004 *Japan. J. Appl. Phys.* **43** 1527
- [15] Yang Y S, Lee S J, Kim S H, Chae B G and Jang M S 1997 *Japan. J. Appl. Phys.* **36** 749
- [16] Kim S-T, Kim H-H, Lee M-Y and Lee W-J 1997 *Japan. J. Appl. Phys.* **36** 294
- [17] Miller S L, Nasby R D, Schwank J R, Rodgers M S and Dressendorfer P V 1990 *J. Appl. Phys.* **68** 6463
- [18] Miller S M, Schwank J R, Nasby R D and Rodgers M S 1991 *J. Appl. Phys.* **70** 2849